

# Quantifying *Geometric* Entanglement: the Linking Number of Two Open Curves

Klint Qinami, Eitan Grinspun

May 15, 2017

## 1 Motivation and Vision: Shape Autophilia

Consider bending a piece of wire into a certain shape. For example, we can bend it to make a paper clip, a spiral, a helix, or we can just keep it unbent, as a straight line segment. How likely is the bent wire to become entangled with similarly bent wires? In other words, what is the propensity of that shape to become entangled? Where does it rank in the spectrum of autophilia, or self-attraction?

We can make this question concrete with a laboratory experiment. Suppose we bend many wires into identical shapes (e.g., many helices of the same chirality, torsion, and length), place these indistinguishable objects into a box, and shake vigorously. If we then pull one object out of the box, how many others will “come along for the ride?” We could count the members of the entangled cluster, return the cluster to the box, vigorously shake again, and then repeat these steps, and in this way produce a histogram of the distributions of the cardinality of the clusters, as one possible measure of the shape’s autophilia.

Understanding how the shape of an object influences its propensity for become entangled is a fundamental question which is interesting in its own right, and also has applications to diverse fields: materials designed from nanostructures or polymers, granular media with non-convex grains, and engineered fibrous structures. Biological systems also harness shape autophilia. Helical strands of hair entangle to form wisps and locks. When a fire ant colony floods, the ants entangle together to form a resilient raft.



Figure 1: Human hair forms wisps and locks. Credits: Eden Arringspun



Figure 2: Wire bent into different shapes. Credits: Hinterdobler.

We would like to define measures of shape autophilia in a manner that is on the one hand amenable to mathematical investigation, and on the other hand relevant to applications.

Our approach will be to carry out a purely theoretical investigation of the definition and properties of shape autophilia. We will interact with computer scientists such as Alec Jacobson (U. Toronto) to interweave this theoretical investigation with computational approaches, including both stochastic numerical optimization and numerical dynamics simulations, to verify and validate the theoretical findings, and to create a stepping stone toward applications. Finally, we will interact with experimentalists such as Stephen Morris (U. Toronto) and Pedro Reis (EPFL) to test the theory and simulations against laboratory experiments.

As a first step, we propose to investigate a generalization of the linking number between two curves. The linking number has been classically defined for two closed curves. In this setting, it is always an integer value and a topological invariant. Physically speaking, two closed curves will always remain either linked, or unlinked, so long as the shapes deform without breaking, since real materials cannot pass through each other.

We will generalize the linking number to two open curves. In this new setting, the linking number is no longer a topological invariant, and no longer restricted to the integers. Instead, the generalized linking number will be a real number that is geometry-dependent. At first glance, the lack of topological invariance would make it seem that this generalized linking number may both less fundamental and less interesting. Yet, such a generalization has the potential to address an important question in the physical world. When open curves can be smoothly moved or deformed, without cutting and without passing through each other, they can become more or less entwined, and we need a continuous measure for this geometry-dependent entwinement between the two open curves.

*The proposed work on the linking number is based on a preliminary (unpublished) investigation with Klint Qinami, third-year undergraduate at Columbia University.*



Figure 3: Staples as a cohesive granular medium. From Nick Gravish, Scott V. Franklin, David L. Hu, and Daniel I. Goldman, *Physical Review Letters*, 108, 208001 (2012).



Figure 4: Fire ants entangle into a cluster to build a raft. Credits: David Hu and Nathan J. Mlot.r



Figure 5: The fire ant raft remains cohesive under external stresses. Credits: David Hu and Nathan J. Mlot.

## 2 Background: Linking Number

Our investigation naturally begins as a search for a mathematical measure of the entanglement of curves in space. Due to the difficulty of the general question of an arbitrary number of curves with arbitrary shape, we initially narrow the parameter space to the entanglement of two closed curves. For this narrower problem there exists an elegant and simple measure, the linking number. Intuitively, this topological invariant measures the ‘number of times’ one curve ‘loops around’ the other.

There exist different formalizations of the linking number; Renzo and Nipoti [2011] recount Gauss’s derivation and prove its equivalence to modern perspectives. To speak of each link component, let  $\gamma_1(t_1), \gamma_2(t_2)$  be two closed curves in  $\mathbb{R}^3$  that are nowhere crossing with  $t_1, t_2 \in [0, 2\pi]$ . To each point  $(t_1, t_2)$  can be associated a unique point on the torus  $\mathbb{T}$ . Define the Gauss Map  $\Gamma : \mathbb{T} \rightarrow S^2$  by

$$\Gamma(t_1, t_2) = \frac{\gamma_1(t_1) - \gamma_2(t_2)}{|\gamma_1(t_1) - \gamma_2(t_2)|}$$

The first formalization of the linking number, due to Gauss, is as the signed area of the image of the Gauss map divided by area of the unit sphere. This can be expressed as

$$L(\gamma_1, \gamma_2) = \frac{1}{4\pi} \int_{\mathbb{T}} \Gamma \cdot \left( \frac{\partial \Gamma}{\partial t_1} \times \frac{\partial \Gamma}{\partial t_2} \right) dT$$

Gauss’s method is simple to state, but practically it is difficult to compute. We therefore shift our point of view to the more modern knot-theory perspective of the linking number.

This perspective is all about perspectives. Let  $\pi_n$  be a projection map onto the plane whose normal vector is  $n$ . Let  $\pi_n(\gamma_1, \gamma_2)$  denote the projection of  $\gamma_1, \gamma_2$ . Suppose the projection is non-degenerate, giving a well-defined, oriented link diagram with over-under crossings. For each crossing, assign  $\pm 1$  according to the right-hand-rule. The sum of all crossings of  $\pi_n$  is twice the linking number.

The equivalence of the two formalizations is seen by equating both definitions to the number of times the torus wraps around the sphere under the Gauss map. Since the degree of a continuous map is homotopy invariant, the linking number must be as well.

## 3 Background: other generalizations of linking number

Various generalizations of the linking number to other closed structures have been considered. The signed area ratio perspective generalizes naturally to closed higher dimensional manifolds, see, e.g., [Shonkwiler 2011]. Closed framed curves (framed knots) have a

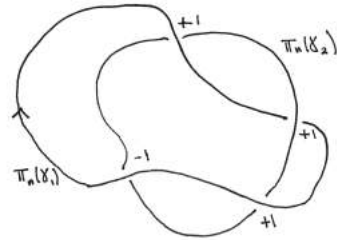


Figure 6: Valid projection with linking number 1.

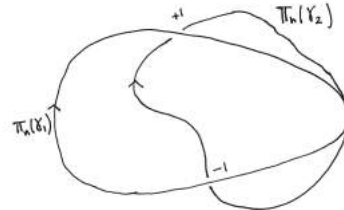


Figure 7: Degenerate projection.

self-linking number that can be computed as the linking number of the knot with a copy of itself displaced along the framing vectors. If the frame is induced by the blackboard framing (normal to the blackboard) then this is called Kauffman’s self-linking number.

The linking number describes the linking of a pair of closed curves, but it cannot see links that are not evident pair-wise. For example, any two components of the Borromean rings have linking number zero, but the three curves are linked. The Milnor invariants capture such links between three or more closed curves [Milnor 1954].

The linking number has been generalized to open curves with fixed/prescribed endpoints, such as to  $n$ -tangles, proper embeddings of the disjoint union of  $n$  arcs into a 3-ball, such that endpoints of the arcs map to  $2n$  prescribed points on the ball’s boundary [Conway 1970]. White’s formula expresses the linking number of two closed curves as the sum of two integrals, the twist and writhe. The writhe of non-closed curves has been defined by either fixing their endpoints [Berger and Prior 2006] or connecting their Gaussian image of their endpoints with a geodesic [Starostin 2005].

The winding number of a closed planar curve or surface in  $\mathbb{R}^3$  counts the number of times that the manifold winds around a given point. Jacobson et al. [2013] generalized the winding number to open planar curves and open surfaces in  $\mathbb{R}^3$ , and demonstrated that the generalization provides a foundation for numerical algorithms that can robustly process geometric data that has noise, gaps, or holes.

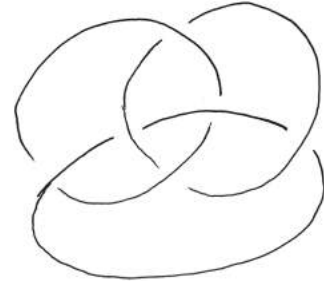


Figure 8: Borromean rings.

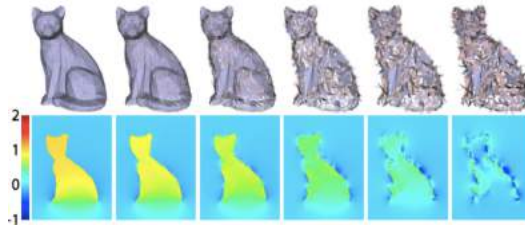


Figure 9: The generalized winding number of Jacobson et al. [2013] allows for robust numerical codes. In this example, each triangular facet in a mesh discretization of a cat (with open bottom) is ripped off and slowly rotated in a random direction, to demonstrate that the generalized winding number gracefully degrades. Credits: Jacobson, Kavan, Sorkine-Hornung [2013].

## 4 Generalized linking number as area ratio

Gauss’s integral definition of the linking number generalizes naturally to open curves parameterized over the unit interval  $I = [0, 1]$ ; we simply replace the toroidal domain by the unit square. Let  $\gamma_1(t_1), \gamma_2(t_2)$  be two open curves in  $\mathbb{R}^3$  that are nowhere crossing, with  $t_1, t_2 \in I$ . The Gauss Map  $\Gamma : I^2 \rightarrow S^2$  has the same expression as before, and the generalized linking

number is given by the ratio of the signed area of the Gaussian image to the area of the unit sphere,

$$L(\gamma_1, \gamma_2) = \frac{1}{4\pi} \int_{I^2} \Gamma \cdot \left( \frac{\partial \Gamma}{\partial t_1} \times \frac{\partial \Gamma}{\partial t_2} \right) dT$$

In generalizing from closed to open curves, the only substantial change we have introduced is that as opposed to the torus, the unit square  $I^2$  has a non-empty boundary. Unlike the torus, the unit square may wrap around the sphere only partially, thus the area ratio  $L(\gamma_1, \gamma_2)$  is not restricted to the integers.

Let us extend the notion of degree to continuous maps such as  $\Gamma : I^2 \rightarrow S^2$ , where the domain has a non-empty boundary but the co-domain has no boundary. In this setting, the degree of the map is no longer one integer, but an integer field  $\text{deg} : S^2 \rightarrow \mathbb{Z}$  over the codomain. For every point  $v \in S^2$  on the codomain, the degree  $\text{deg}(v)$  counts the signed number of times that the image of  $\Gamma$  covers  $v$ .

Furthermore,  $\Gamma$  maps the domain boundary  $\partial I^2$  onto a closed (generally self-intersecting) partition curve  $\delta : S \rightarrow S^2$ , which partitions  $\text{deg}(v)$  into piecewise constant regions. Integrating the degree  $\int_{S^2} \text{deg}(v) dS$  recovers the signed area of  $\text{Im}(\Gamma)$ . The piecewise constant structure of  $\text{deg}(v)$  demarcated by  $\delta$  has can also be interpreted from the perspective of the linking number.

## 5 Generalized linking number as expected linking number

To generalize the linking number to open curves, we again consider projected link diagrams. However, it no longer suffices to pick one regular point of the Gauss map, since different non-degenerate projections can yield different linking numbers. This follows by considering the Hopf Link where a piece of one curve is chopped off. For most projections, the linking diagram computation of this configuration is indistinguishable from the Hopf Link, since only intersections are computationally considered in the link diagram. However, the fact that this link is not the Hopf Link can be determined when an intersection is missing, due to one curve projecting onto the chopped-off portion of the other curve.

Averaging the result of these linking diagrams over all points in the image of the Gauss map gives the expected linking number over all projections. For closed curves, this is just the integer linking number, since all non-degenerate projections yield the same linking number. For open curves, in general, the linking number no longer yields an integer, and the sum of

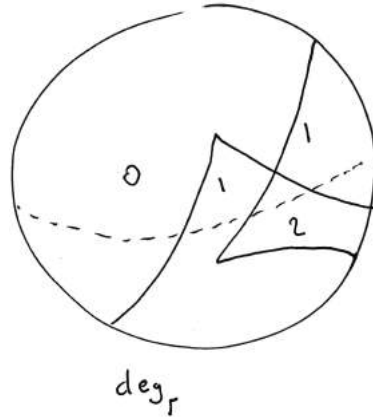


Figure 10: Image of unit square on the unit sphere. Numbers represent degree of region.

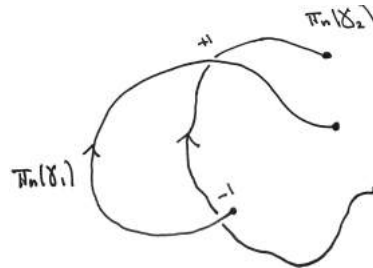


Figure 11: Example projection for open curves.

all intersections for each linking diagram is no longer guaranteed to be an even number by the Jordan Curve Theorem.

Consider those projections where the endpoint of one curve and some point on the other curve both project to the same point on the plane. Such projections form the closed (generally self-intersecting) loop  $\delta$  on the sphere. This can be seen as the image of the boundary of the domain of the Gauss map. This boundary corresponds to the tipping point between losing or gaining an intersection — in other words, a change in the linking number computation. Hence this curve partitions the sphere into pieces where the linking number is constant. Additionally, adjacent separate regions on the sphere must differ by exactly  $\frac{1}{2}$ .

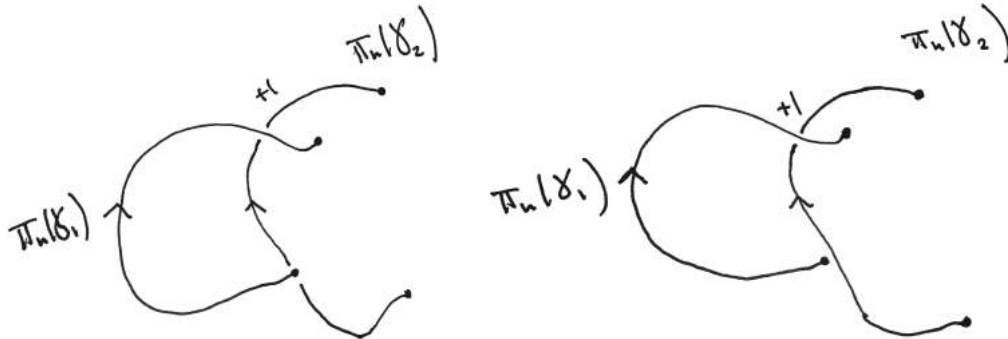


Figure 12: *Left:* Endpoint of one curve on top of the other curve. *Right:* Transition of endpoint causing removal of intersection.

## 6 Gradient of linking number as area gradient

Observe that the generalized linking number is no longer homotopy invariant. Smooth deformations of  $\gamma_i$  vary the position of the partition curve  $\delta$  and the area of  $\text{Im}(\Gamma)$ . Why continue along this road if we lose topological invariance? Because now we can deliberately change the linking number through homotopy.

This partition curve  $\delta$  is fundamental for numerical optimization of the linking number, since it sections off regions with different linking numbers. Hence maximizing the total linking number corresponds to increasing the area of the regions with the largest linking number. Because these regions are ultimately determined by the positions of curves in space, we can determine the chain effect that moving these curves has on the regions, and optimize curve positions to increase the linking number by making the regions larger.

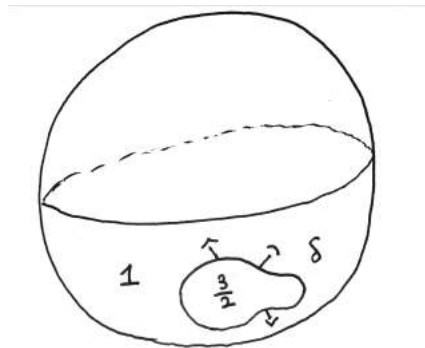


Figure 13: Area gradient of region enclosed by partition curve.

## 7 Discretization and Numerical Computation

Curves in Euclidean space are readily discretized by a finite sequence of vertices (discrete points) connected by straight line segments. If  $\gamma(t) : I \rightarrow \mathbb{R}^3$  is a smooth space curve, then partition the unit interval by points  $0 = t_0 < t_1 < \dots < t_n = 1$  and consider the piecewise linear path given by the union of all maps  $[t_k, t_{k+1}] \mapsto [\gamma(t_k), \gamma(t_{k+1})]$ , where  $[\gamma(t_k), \gamma(t_{k+1})]$  denotes the straight line segment connecting the two points. As the  $\max_k |t_{k+1} - t_k|$  of the partition goes to zero, sufficiently smooth curves are recovered exactly.

To pick projection planes, we first approximate the unit sphere by using recursive subdivision of the faces of a regular icosahedron for an isotropic layout. For each vertex  $w_i$  of the polyhedron, we use a change of basis matrix to get  $u_i, v_i, w_i$  coordinates for each vertex of the polyline, where  $\{u_i, v_i\}$  are an orthonormal basis for the plane normal to  $w_i$ . Each  $u_i v_i$  plane gives a linking diagram. If numerical issues are encountered when determining intersections of the link diagram, the computation of the linking number of this diagram is thrown out of the averaging and the projection direction is considered degenerate. Since the image of the critical set of a smooth map has measure zero, these degenerate projections do not affect the average in the limit.

The partition curve  $\delta$  is discretized by computing the normals given by the endpoint of one curve and a vertex of the other. If  $\gamma_0, \gamma_1$  are two curves and  $t_0, \dots, t_n$  is a partition of  $I$ , then discrete vertices on the partition curve are

$$\frac{\gamma_i(\{0, 1\}) - \gamma_{1-i}(t_k)}{|\gamma_i(\{0, 1\}) - \gamma_{1-i}(t_k)|}$$

These vertices are then connected by great circles, preserving orientation, giving a spherical loop that may self-intersect. Each closed piece of the loop is a spherical polygon, whose area is given by the classical angle defect formula

$$A = (2 - n)\pi + \sum_i \phi_i$$

where  $n$  is the number of vertices of the polygon and each  $\phi_i$  is an interior angle. This formula can be differentiated with respect to the vertex positions of the curves in space, and this informs the numerical optimization — move vertices to increase the interior angles.

$$\nabla A = \sum_i \nabla \phi_i$$

Since each interior angle is a function of the vertex positions of  $\delta$ , which are determined by the positions of  $\gamma_0, \gamma_1$ , this area gradient informs how make  $\gamma_0, \gamma_1$  more or less linked.

## 8 Preliminary Implementation

To test our discretization and evaluate the merit of this approach, we have developed a preliminary numerical implementation of the generalized linking number computation. Our

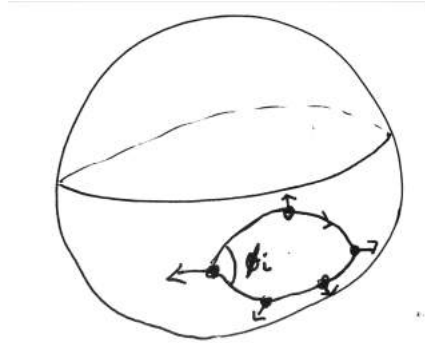


Figure 14: Area gradient of spherical polygon enclosed by discrete partition curve.

preliminary test of this code considered an “Open Hopf Link,” where the one curve has a gap. Figure 15 depicts our discretization of the Open Hopf Link. The two curves are given by  $\gamma_1(t) = (\cos(t), \sin(t), 0)$  and  $\gamma_2(t) = (0, \cos(t) + 1, \sin(t))$  for  $t \in [0, 2\pi]$ . The partition width displayed is uniformly  $2\pi/50$ . The link is open since  $\gamma_2$  is an open curve, as the final line segment  $[\gamma(t_{49}), \gamma(t_{50})]$  is removed. When we visualize the image of the Gauss map for the Open Hopf Link, the partition curve and piecewise constant degree of the map becomes evident.

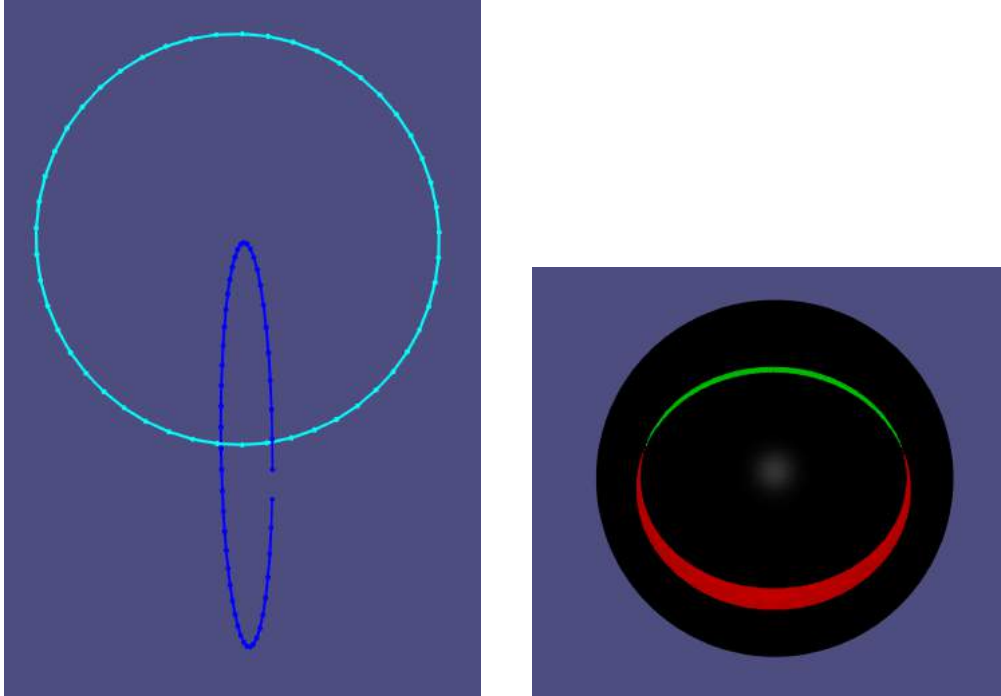


Figure 15: *Left:* An “Open Hopf Link” discretization. *Right:* Image of the Gauss map, color coded by linking number, equivalently Gauss map degree: (black = 1, green =  $\frac{3}{2}$ , red =  $\frac{1}{2}$ ).

## 9 Open questions

The generalized linking number is a promising tool in tackling the general question of what shapes are *most likely* to become (dis)entangled, *and how* to manipulate shapes (via rigid motions, or flexible deformations) to (dis)entangle them. Questions abound:

1. Does the gradient of the generalized linking number effectively guide the process of disentangling two curves?
2. For framed knots, we can consider the self-linking number of the knot—the linking number of the knot with a version of itself translated infinitesimally along its frame. This self-linking number can be generalized analogously. Does the generalized self-linking number accurately predict the propensity of a curve to form knots?

3. Among all smooth curves subject to some limits (e.g., fixed length, maximum curvature), which have the largest self-linking number? Given one smooth curve  $\gamma_1$ , among all smooth curves  $\gamma_2$  subject to some limits, which has the largest linking number with respect to  $\gamma_1$ ?
4. Given two open curves with known “coarse” measurements (total length, average curvature and curvature variance, etc.) randomly placed in the unit sphere, what is the *expected* expected linking number?
5. Consider the stochastic experiment presented earlier, taking many identically shaped curves, placing and shaking them in a box, and computing the expected clump size through experimental trials. Can the clump size be predicted using the generalized linking number directional derivative with respect to rigid motions (translations and rotations)?
6. What is the relationship between a curve’s propensity to entangle versus disentangle?
7. Can the generalized linking number be extended to nontrivial links like the Whitehead link?
8. What other tools are necessary to fully characterize shape autophilia?

## References

- [1] Mitchell A Berger and Chris Prior. The writhe of open and closed curves. *Journal of Physics A: Mathematical and General*, 39(26):8321, 2006.
- [2] John H Conway. An enumeration of knots and links, and some of their algebraic properties. In *Computational Problems in Abstract Algebra (Proc. Conf., Oxford, 1967)*, pages 329–358, 1970.
- [3] Alec Jacobson, Ladislav Kavan, and Olga Sorkine-Hornung. Robust inside-outside segmentation using generalized winding numbers. *ACM Transactions on Graphics (TOG)*, 32(4):33, 2013.
- [4] John Milnor. Link groups. *Annals of Mathematics*, 59(2):177–195, 1954.
- [5] Renzo L Ricca and Bernardo Nipoti. Gauss’linking number revisited. *Journal of Knot Theory and Its Ramifications*, 20(10):1325–1343, 2011.
- [6] Clayton Shonkwiler and David Shea Vela-Vick. Higher-dimensional linking integrals. 2008.
- [7] E Starostin. On the writhing number of a non-closed curve. World Scientific Publishing, 2005.